

# Geomagnetic Reversals Caused by Breaking Mirror Symmetry of Core Dynamics

François Pétrélis,<sup>1</sup> S. Fauve,<sup>1</sup> Emmanuel Dormy,<sup>2,3</sup> and Jean-Pierre Valet<sup>3</sup>

<sup>1</sup>*Laboratoire de Physique Statistique de l'Ecole Normale Supérieure,  
CNRS UMR 8550, 24 Rue Lhomond, 75231 Paris Cedex 05, France*

<sup>2</sup>*Laboratoire de Radio-Astronomie, Ecole Normale Supérieure, 24 rue Lhomond, 75005, Paris, France.*

<sup>3</sup>*Institut de Physique du Globe de Paris, 4, Place Jussieu, F-75252 Paris Cedex 05, France.*

(Dated: June 30, 2022)

The Earth's magnetic field can be geometrically described by a strong axial dipole and higher degree terms, which belong to the dipolar (even) or quadrupolar (odd) family depending on their symmetry with respect to the equatorial plane. It is established that the field has frequently (and maybe always) reversed its polarity. It has been suggested by Merrill and Mc Fadden [1] that reversals occur because the fluid flow in the outer core breaks the equatorial symmetry. This results in a coupling between the dipolar and quadrupolar families. Field reversals have now been reported in several numerical simulations of dynamos and very recently for the first time in a laboratory experiment involving a Von Karman swirling flow of liquid sodium (VKS) [2]. In this experiment, reversals are observed when the velocities of the two counter rotating disks driving the flow are different, thus when a symmetry is broken. Here, we show how the interaction between the dipolar and quadrupolar modes, that results from such lack of symmetry, can lead to polarity reversals or excursions. We identify the mechanism at work and discuss its consequences on the shape of reversals and excursions, and the existence of long periods of time without reversals. We then test the predictions of the model with the characteristics of reversals obtained from the paleomagnetic records as well as from the laboratory experiment.

PACS numbers:

## INTRODUCTION

The different modes of the Earth's magnetic field can be classified as follows: dipolar modes are the ones unchanged by mirror symmetry,  $\mathbf{D} \rightarrow \mathbf{D}$ , whereas quadrupolar modes change sign,  $\mathbf{Q} \rightarrow -\mathbf{Q}$  (Figure 1a). The VKS experiment involves a flow of liquid sodium generated by two coaxial counter-rotating iron impellers in a cylindrical volume. When the impellers counter-rotate fast enough at the same frequency, a magnetic field with a dominant axial dipole component is generated (Figure 1b) [3, 4]). A key observation is that time dependent regimes of the magnetic field including polarity reversals are observed only when the impellers rotate at different frequencies [2]. Although the symmetry of the VKS experiment differs from that of the Earth's core, dipolar and quadrupolar modes can be also defined: dipolar modes are the ones that change sign when a rotation of angle  $\pi$  is performed about any axis in the mid-plane between the impellers,  $\mathbf{D} \rightarrow -\mathbf{D}$ , whereas quadrupolar modes are unchanged,  $\mathbf{Q} \rightarrow \mathbf{Q}$  (Figure 1b).

One can write (both for Earth and VKS) any magnetic field as

$$\mathbf{B}(r, t) = d(t)\mathbf{D}(r) + q(t)\mathbf{Q}(r), \quad (1)$$

where  $d(t)$  and  $q(t)$  are the amplitudes of eigenmodes with dipolar and quadrupolar symmetry, respectively. Close to the dynamo threshold,  $d(t)$  and  $q(t)$  are governed by equations of the form,

$$\dot{d} = \alpha d + \beta q + \dots, \quad \dot{q} = \gamma d + \delta q + \dots, \quad (2)$$

where dots stand for higher order terms). Since the dipolar and quadrupolar modes are transformed in a different way by mirror symmetry in the case of the Earth or by rotation of  $\pi$  in VKS, they cannot be linearly coupled when these symmetries are met, thus  $\beta = \gamma = 0$ . This is no longer true otherwise. For simplicity, we define

$$A = d + iq = R \exp(i(\theta + \theta_0)), \quad (3)$$

with  $\theta_0$  such that  $\nu \exp(-2i\theta_0) = \rho$  is real, where the real and imaginary parts of  $\mu$  and  $\nu$  are given by  $2\mu_r = \alpha + \beta$ ,  $2\mu_i = \gamma - \beta$ ,  $2\nu_r = \alpha - \delta$ ,  $2\nu_i = \gamma + \beta$ . We assume that the nonlinear terms saturate the amplitude  $R$  to a finite value [5]. The imaginary part of the equation for  $\dot{A}$  then gives

$$\dot{\theta} = \mu_i - \rho \sin 2\theta. \quad (4)$$

When the flow is perfectly symmetric (i.e. either when the flow in the Earth core displays equatorial symmetry or when the two impellers of the VKS experiment rotate at same frequency)  $\mu_i = 0$ . Then for  $\alpha$  positive, the system has two stable dipolar solutions (corresponding to both polarities). For  $0 < \gamma < \alpha$ , two quadrupolar modes are also solutions, but they are unstable to a dipolar perturbation. When the symmetry of the flow is broken,  $\mu_i$  is different from zero and this can strongly modify the behavior of the solution of the above equations. For  $\mu_i$  smaller than  $\rho$ , four solutions exist:  $\theta_c$  and  $\pi + \theta_c$  are stable solutions while  $\pi/2 - \theta_c$  and  $3\pi/2 - \theta_c$  are unstable ( $2\theta_c = \arcsin(\mu_i/\rho)$ ). Random initial conditions are attracted toward one of the two stable solutions (Fig. 2a). They now correspond to mixed modes, which evolve away from the purely dipolar mode, with increasing quadrupolar contribution when  $\mu_i$  is increased (i.e. as the flow departs from the original symmetry). The non-symmetric part of the flow induced a field with quadrupolar symmetry from the dipolar mode  $\mathbf{D}$ . In general, this quadrupolar field has a non vanishing projection on  $\mathbf{Q}$ . This results in the mixed mode described above. During this process the unstable solution also evolves away from the purely quadrupolar mode and involves an increasing amount of dipolar component. For  $\mu_i = \rho$ , a bifurcation occurs: each stable solution collides with an unstable solution and disappears. This is a saddle-node bifurcation [6] that generates a limit cycle (thus an oscillatory magnetic field) for  $\mu_i > \rho$  (Fig. 2b). Usually, saddle-node bifurcations involve only one stable and one unstable fixed point. Here the problem being invariant under  $\mathbf{B} \rightarrow -\mathbf{B}$  yields the existence of two pairs of stable and unstable fixed points that simultaneously collide at the threshold of the saddle-node bifurcation. This scenario is not restricted to the equation for  $\theta$  that we have considered here. We expect that the interaction between two linearly coupled modes generically displays this bifurcation [5]. Similar equations have been studied in a variety of problems. This has been done for instance for the orientation of a rigid rotator subject to a torque [7]. It was introduced as a toy model for the coupling between the toroidal and the poloidal field of a single dynamo mode. Indeed, symmetries constrain the form of the equation for  $\theta$  even though the modes and the physics involved are different.

### FLUCTUATIONS IN THE VICINITY OF THE BIFURCATION (REVERSALS, EXCURSIONS...)

So far, we did not consider possible effects of fluctuations. The flow in the Earth's core as well as in the VKS experiment is far from being laminar. We can therefore assume that turbulent fluctuations act as noisy terms in the low dimensional system that describes the coupling between the two magnetic modes. In Figure 2b, the system is below the threshold of the saddle-node bifurcation and in the absence of fluctuation exhibits two stable (mixed) solutions. The solution is initially located close to one of the stable fixed points, say  $Bs$ . Fluctuations can push the system away from  $Bs$ . If it goes beyond the unstable fixed point  $Bu$ , it is attracted by the opposite fixed point  $-Bs$ , and thus achieves a polarity reversal. A reversal is made of two successive phases. The first phase  $Bs \rightarrow Bu$  in Figure 2a is the approach toward an unstable fixed point. The deterministic dynamics act against the evolution and this phase is slow. The second phase  $Bu \rightarrow -Bs$  depicts the evolution from the unstable fixed point toward the opposite stable fixed point  $-Bs$ . At the end of the first phase, the system may return toward the initial stable fixed point (phase  $Bu \rightarrow Bs$ ). This is an excursion. Since the deterministic dynamics favors the motion this phase is fast. Note that  $Bu$  could in principle lie on the opposite side of the quadrupolar axis to  $Bs$ . In this configuration the system would reverse for a very short period and then recover the original polarity. In summary, the paths predicted in Figure 2 describe features clearly observed in paleomagnetic records: intensity lows, excursions and reversals [8, 9, 10].

### PREDICTIONS TESTED AGAINST PALEOMAGNETIC DATA AND THE VKS EXPERIMENT

To take into account the fluctuations, we modify the equation for  $\theta$  into

$$\dot{\theta} = \mu_i - \rho \sin(2\theta) + \Delta \zeta(t), \quad (5)$$

from which we derive the evolution of the dipole by  $D = R \cos(\theta + \theta_0)$ .  $\zeta$  is a Gaussian white noise and  $\Delta$  is its amplitude. We have computed a time series of the dipole amplitude (Figure 3a) for a system below the threshold of the bifurcation ( $\mu_i = 0.8$ ,  $\rho = 1$ ,  $\theta_0 = 0.3$ ) and with noise amplitude  $\Delta = 0.2$ . In Figure 3b we show a time series of the magnetic field measured in the VKS experiment and the composite record of the geomagnetic dipole for the past 2 Myr (Figure 3c). The three curves display very similar behaviors with abrupt reversals and large fluctuations.

One of the most noticeable features common to all curves is the existence of a significant overshoot that immediately follows the reversals. In Figure 4, the enlarged views of the period surrounding reversals and excursions also show that this is not the case for the excursions. In fact, the relative position of the stable and unstable fixed points (Figure 2)

controls the evolution of the field. During the first phase, reversals and excursions are similar, but they differ during the second phase. The synopsis shows that the reversals reach the opposite fixed point from a larger value and thus display an overshoot while excursions do not.

During a reversal, the total magnetic field does not vanish. The time scales involved in the dynamics can thus be different from the characteristic time constants of an infinitesimal magnetic field, which is consistent with the typical short duration of reversals ( $\tau_r \sim 10^3$  yrs [11]) with respect to the diffusive time-scales of the magnetic dipole in the absence of flow ( $\tau_d \sim 10^4$  yrs [12]). Below the onset of bifurcation reversals occur very seldomly, which suggests that their occurrence requires rarely cooperative fluctuations (Figure 2). The evolution from the stable to the unstable fixed point (phase  $Bs \rightarrow Bu$ ) can be described as the noise driven escape of the system from a metastable potential well. The durations of polarity intervals are equivalent to the exit time and are exponentially distributed according to [13]

$$P[T] \propto \exp(-T)/\langle T \rangle. \quad (6)$$

The averaged duration of polarity intervals  $\langle T \rangle$  depends on the fluctuation intensity and on the distance to the saddle-node bifurcation. For the model studied, we obtain

$$\log \langle T \rangle \propto 2 \frac{(2(\rho - \mu_i)/\rho)^{3/2}}{3\Delta^2}. \quad (7)$$

These predictions assume that the noise intensity and the deterministic dynamics do not vary in time. It is likely that the Rayleigh number in the core and the efficiency of coupling processes between the magnetic modes have evolved throughout the Earth history. The exponential dependence of the mean polarity duration  $\langle T \rangle$  on noise intensity implies that a moderate change in convection can result in a very large change of  $\langle T \rangle$ . This might account for changes in the rate of geomagnetic reversals and very long periods without reversals (so called superchrons, see [14, 15]).

Recent numerical simulations of the geodynamo have pointed out the importance of hydrodynamic symmetry breaking during reversals. In [16], reversals of the axial dipole are simultaneous with the increase of the axial quadrupole, when the North-South symmetry of the convective flow is broken. In a similar simulation [17], it has been demonstrated that if the flow or the magnetic field is forced to remain equatorially symmetric, then reversals do not occur.

We note that two modes with the same symmetry can be linearly coupled by an equatorially symmetric flow and display the bifurcation mentioned above. Nevertheless, when a dipolar and a quadrupolar mode are involved, reversals are favored by breaking equatorial symmetry .

## CONCLUSION

We have proposed a scenario for reversals of the magnetic field generated by dynamo action. When the flow breaks its equatorial symmetry, it couples modes with dipolar and quadrupolar symmetries. This coupling drives the system close to a saddle-node bifurcation. The scenario offers a simple and unified explanation for many intriguing features of the Earth magnetic field. The most significant output of the model is that it predicts specific characteristics of the field obtained from paleomagnetic records of reversals and from recent experimental results. Other characteristic features such as intensity lows and excursions as well as the existence of long periods without reversals, can be understood in the same framework.

We have considered the regime below the threshold of the saddle-node bifurcation where fluctuations drive random reversals by excitability. We also point out that above the saddle-node threshold, the solution displays roughly periodic oscillations. It is tempting to link this regime to the evolution of the large scale dipolar field of the Sun (which reverses polarity roughly every 11 years).

- 
- [1] Merrill R.T., Mac Fadden P.L. "Secular Variation and the Origin of Geomagnetic Field Reversals" , Journal of Geophysical Research (93) 11,589-11,597 (1988).  
 [2] Berhanu, M., Monchaux, R., Fauve, S., Mordant, N., Pétrélis, F., Chiffaudel, A., Daviaud, F., Dubrulle, B., Marié, L., Ravelet, F., Bourgoïn, M., Odier, Ph., Pinton, J.-F., Volk, R. "Magnetic field reversals in an experimental turbulent dynamo", Europhys. Lett. (77), 59001 (2007).

- [3] Monchaux, R., Berhanu, M., Bourgoin, M., Moulin, M., Odier, Ph., Pinton, J.-F., Volk, R., Fauve, S., Mordant, N., Pétrélis, F., Chiffaudel, A., Daviaud, F., Dubrulle, B., Gasquet, C. and Marié, L. "Generation of a magnetic field by dynamo action in a turbulent flow of liquid sodium", *Phys. Rev. Lett.* (98), 044502 (2007).
- [4] Pétrélis F, Mordant N, Fauve S., "On the magnetic field generated by experimental dynamos", *Geophysical and Astrophysical Fluid Dynamics* 101:3, 289-323 (2007).
- [5] Pétrélis F. and Fauve S., "Excitability in the vicinity of a saddle-node bifurcation: a mechanism for reversals", (to be submitted 2008).
- [6] Guckenheimer J. and Holmes P. *Nonlinear Oscillations, Dynamical Systems and Bifurcations of Vector Fields*. Springer-Verlag. (1986).
- [7] Hoyng P., "Turbulent transport of magnetic fields" *Astronomy & Astrophysics* (171) 348-356, (1986).
- [8] Valet J.-P., Meynadier L., Guyodo Y., "Geomagnetic field strength and reversal rate over the past 2 Million years". *Nature* 435, 802-805 (2005).
- [9] Channell J.E.T, "Late Brunhes polarity excursions (Mono Lake, Laschamp, Iceland Basin and Pringle Falls) recorder at ODP Site 919 (Irminger Basin)", *Earth Planet. Sci. Lett.* 244, 378-393 (2006).
- [10] Valet J.-P., Plenier G. and Herrero-Bervera E., "Geomagnetic Excursions reflect an aborted polarity state", *Earth Planet. Sci. Lett.* (in press 2008).
- [11] Valet J.-P. and Herrero-Bervera E., "Geomagnetic Reversals, archives", *Encyclopedia of Geomagnetism and Paleomagnetism*, 339-346, D. Gubbins and E. Herrero-Bervera Eds., Springer (2007).
- [12] Moffatt H.K. "Magnetic Field Generation in Electrically Conducting Fluids", Cambridge University Press. (1978).
- [13] Van Kampen N. G. *Stochastic Processes in Physics and Chemistry*. Elsevier. (1992).
- [14] Lowrie W., "Geomagnetic polarity timescales", *Encyclopedia of Geomagnetism and Paleomagnetism*, 328-333, D. Gubbins and E. Herrero-Bervera Eds., Springer (2007).
- [15] Hulot G., Gallet Y., "Do superchrons occur without any paleomagnetic warning ?", *Earth Planet. Sci. Lett.* (210) 1-2, 191-201 (2003).
- [16] Li J., Sato T. and Kageyama A., "Repeated and sudden reversals of the dipole field generated by a spherical dynamo action", *Science* (295), 1887 (2002).
- [17] Nishikawa N. and Kusano K., "Simulation study of the symmetry-breaking instability and the dipole field reversal in a rotating spherical shell", *Physics of Plasma*, submitted (2008).

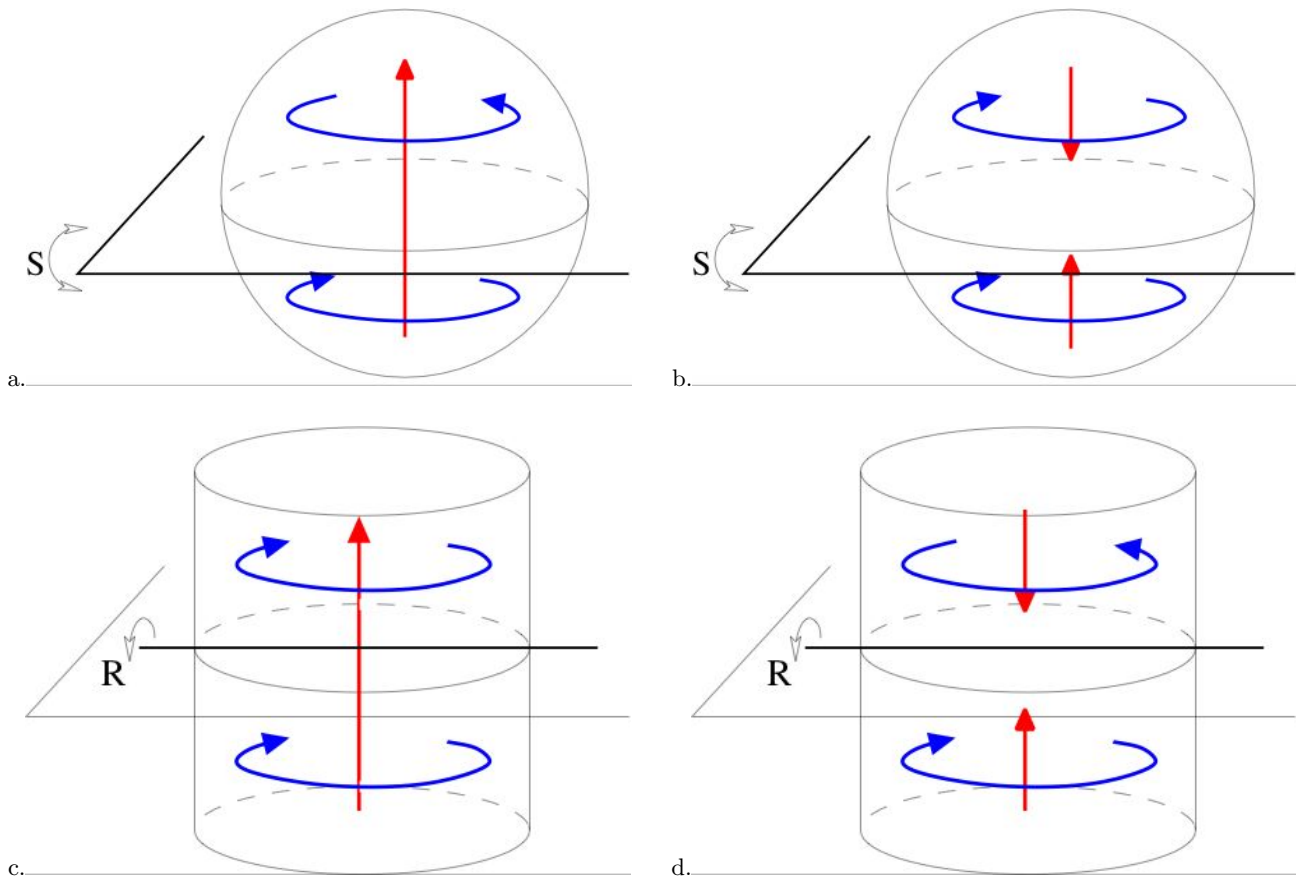


FIG. 1: Magnetic modes with (a & c) dipolar, (b & d) quadrupolar symmetry in the Earth (a & b) and the VKS experiment (c & d). Poloidal (red) and toroidal (blue) components of the magnetic field.

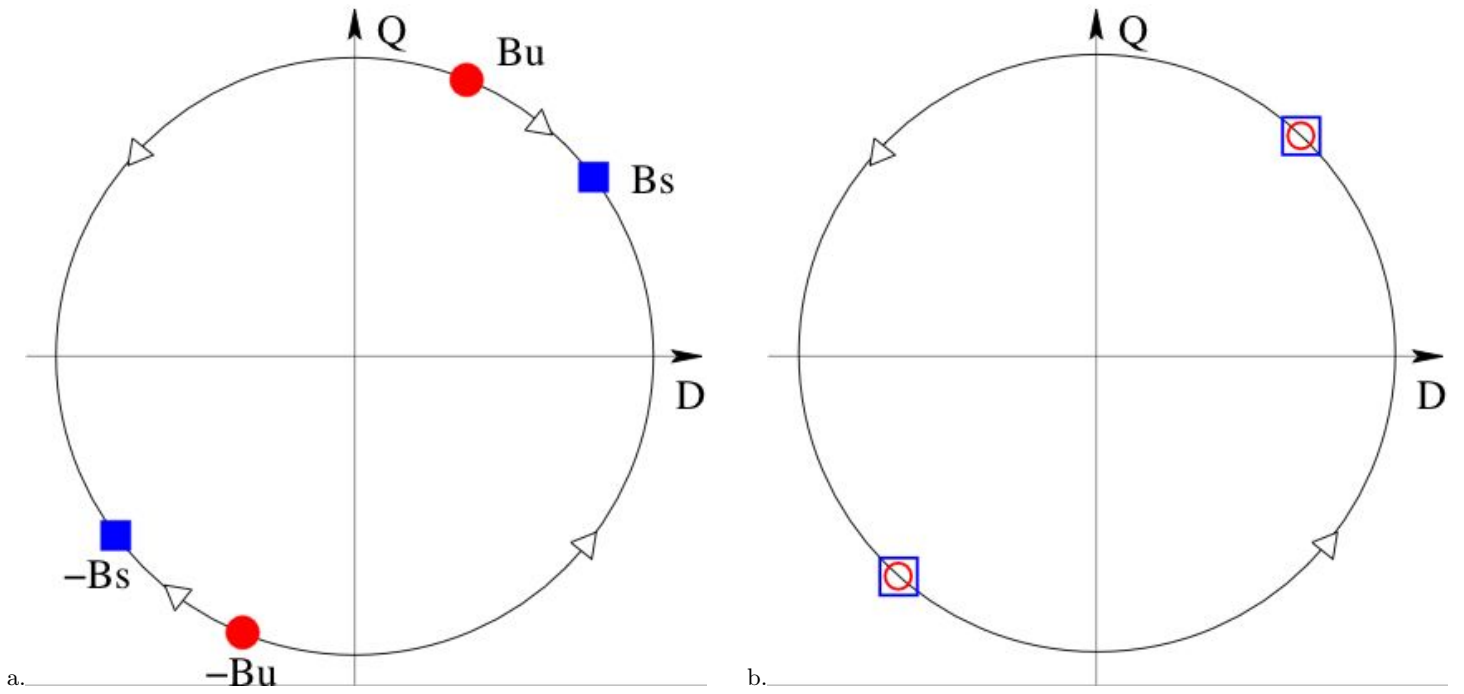


FIG. 2: Phase space of a system invariant under  $\mathbf{B} \rightarrow -\mathbf{B}$  and displaying a saddle-node bifurcation. **a:** below the onset of the saddle-node bifurcation, (square blue): stable fixed points; (red circle): unstable fixed points. **b:** above the onset of bifurcation, the fixed points (empty symbols) have collided and disappeared, the solution describes a limit cycle. Note that in a, below the onset of the saddle-node bifurcation, fluctuations can drive the system from  $Bs$  to  $Bu$  (phase  $Bs \rightarrow Bu$ ) and initiate a reversal (phase  $Bu \rightarrow -Bs$ ) or an excursion (phase  $Bu \rightarrow Bs$ ).

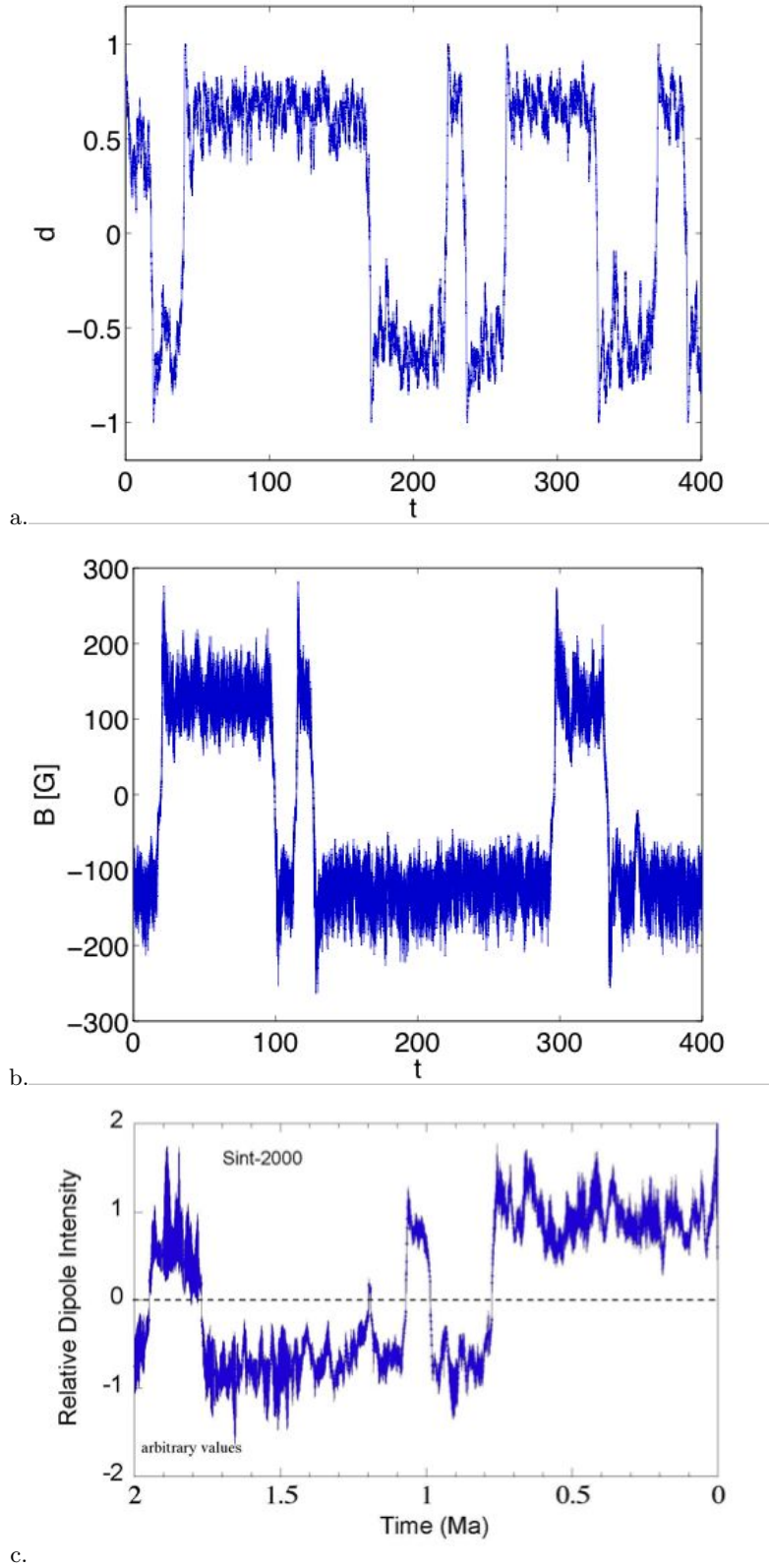


FIG. 3: **a:** Time series of the dipole amplitude for a system below the threshold of the bifurcation,  $\mu_i = 0.9$ ,  $\rho = 1$ ,  $\theta_0 = 0.3$  and with noise amplitude  $\Delta = 0.2$ . **b:** Time series of the magnetic field measured in the VKS experiment for the two impellers rotating with different frequencies  $F_1=22$  Hz,  $F_2=16$  Hz, data from [2]. **c:** Composite paleointensity curve for the past 2 millions years, present corresponds to  $t=0$ , data from [8].

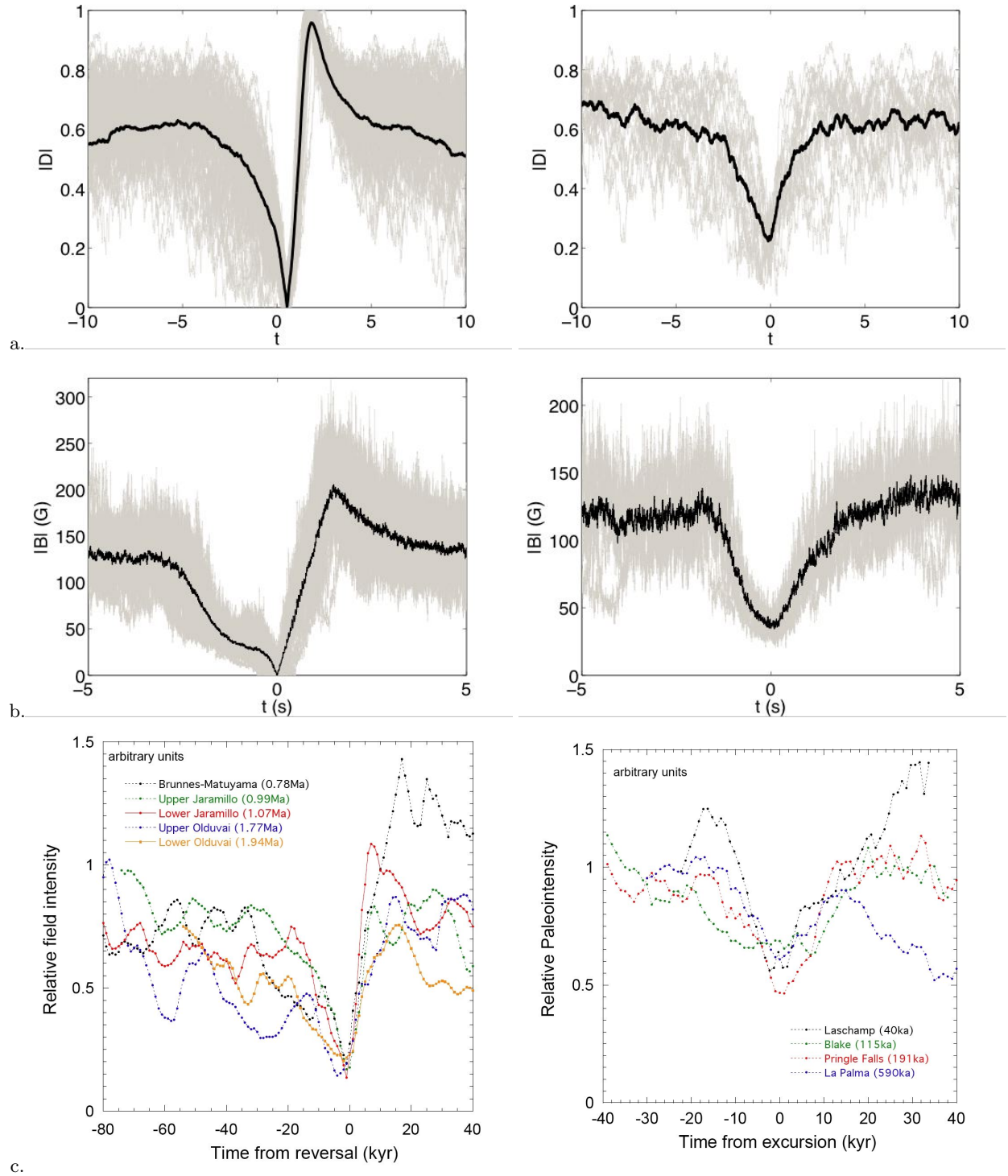


FIG. 4: Comparison of reversals and excursions in the solutions of the equation for  $\theta$  (a), the VKS experiment (b) (data from [2]), and in paleomagnetic data (c) (data from [8]). Black curves in (a) and (b) represent the averaged curve, each realization being represented in grey.